INL/CON-08-14243
PREPRINT

Jacobian-Free Newton Krylov Discontinuous Galerkin Method and Physics-Based Preconditioning for Nuclear Reactor Simulations

International Conference on Reactor Physics, Nuclear Power: A Sustainable Resource

HyeongKae Park
Robert R. Nourgaliev
Richard C. Martineau
Dana K. Knoll

September 2008

This is a preprint of a paper intended for publication in a journal or proceedings. Since changes may be made before publication, this preprint should not be cited or reproduced without permission of the author. This document was prepared as an account of work sponsored by an agency of the United States Government. Neither the United States Government nor any agency thereof, or any of their employees, makes any warranty, expressed or implied, or assumes any legal liability or responsibility for any third party's use, or the results of such use, of any information, apparatus, product or process disclosed in this report, or represents that its use by such third party would not infringe privately owned rights. The views expressed in this paper are not necessarily those of the United States Government or the sponsoring agency.

The INL is a
U.S. Department of Energy
National Laboratory
operated by
Battelle Energy Alliance

International Conference on Reactor Physics, Nuclear Power: A Sustainable Resource
Casino-Kursaal Conference Center, Interlaken, Switzerland, September 14-19, 2008

Jacobian-free Newton Krylov discontinuous Galerkin method and physics-based preconditioning for nuclear reactor simulations

HyeongKae Park*, Robert R. Nourgaliev, Richard C. Martineau, Dana A. Knoll

Idaho National Laboratory
Multiphysics Methods Group
2525 North Fremont Ave.
Idaho Falls, Idaho 83415-3860, USA

Abstract

We present a high-order-accurate spatiotemporal discretization of an all-speed flow solver using Jacobian-free Newton Krylov framework. One of the key developments in this work is the physics-based preconditioner for the all-speed flow, which makes use of traditional semi-implicit schemes. We use the fully conservative formulation of the Navier-Stokes equations, but precondition these equations in the primitive variable form, which allows for a straightforward separation of physical phenomena. Numerical examples demonstrate that the developed preconditioner effectively reduces the number of the Krylov iterations, and the efficiency is independent of the Mach number and mesh sizes under fixed CFL conditions.

1. Introduction

Multidimensional, higher-order (2^{nd} and higher) numerical methods have come to the forefront in recent years due to significant advances of computer technology and numerical algorithms, and have shown great potential as viable design tools for realistic applications. To achieve this goal, *fully implicit high-order* accurate coupling of the physics is a critical component.

One of the issues that arise from multiphysics simulations is the necessity to resolve multiple time scales. For example, the dynamical time scales of neutron kinetics, fluid dynamics and heat conduction significantly differ (typically $> 10^{10}$ magnitude), with the dominant (fastest) physical mode significantly changing during the course of transient (Pope and Mousseau, 2007). This leads to the severe time step restriction for stability in traditional multiphysics (i.e., operator split, semi-implicit discretization) simulations. The lower order methods suffer from an undesirable excessive numerical dissipation. Thus implicit, higher order accurate scheme is necessary to perform seamlessly-coupled multiphysics simulations that can be used to analyze the "what-if" regulatory accident scenarios, or to design and optimize engineering systems.

The high-temperature gas-cooled nuclear reactor concepts have fundamental differences from the conventional light water reactors (LWR), and

* Corresponding author, Ryosuke.Park@inl.gov Tel: +1 (208) 526 9502; Fax: +1 (208) 526 2930.

the nominal operational conditions are expected to be at higher thermal loadings. Under high heat flux conditions, density variations in the coolant become significant. In these regimes, the "traditional approaches" (i.e., incompressible flow simulations with the Boussinesq approximation for buoyancy) may cease to be valid. An example of this effect was reported by the work of Darbandi and Hosseinizadeh (Darbandi and Hosseinizadeh, 2007), where greater than 10% difference in the local Nusselt number has been observed. Therefore, development of more appropriate numerical methods based on the fully conservative and compressible formulation is necessary to eliminate deficiencies of the "traditional approaches".

In this work, the Discontinuous Galerkin (DG) method for all-speed fluid flow is incorporated into the Jacobian-free Newton-Krylov (JFNK) framework (Knoll and Keyes, 2004). Advantages of combining the DG with the JFNK are two-fold: *a)* enabling *robust and efficient high-order-accurate modelling of all-speed flows on unstructured grids*, thus opening the possibility for high-fidelity simulation of nuclear power relevant flows; and *b)* the ability to *tightly and robustly couple other relevant physics* (i.e. neutronics, thermal-structural response of solids) in a high-order accurate manner. In the present study, we focus on the physics-based preconditioning (PBP) of the Krylov method (GMRES), used as the linear solver in our implicit time discretization scheme.

2. JFNK-DG framework

2.1. Discontinuous Galerkin method

The Discontinuous Galerkin (DG) method can be thought of as a higher order extension of the finite volume (FV) method that utilizes the Galerkin finite element framework. The FV has long been the main vehicle for solving hyperbolic conservation laws. Its (relatively) simple formulation can be easily extended to multi-dimensions; however, the higher order accurate FV requires wide stencils, which may become very cumbersome for the multidimensional unstructured grids as well as the treatment of the boundary conditions, parallelization, and adaptive mesh refinement (Cockburn et al., 1990). The DG, on the other hand, makes use of the orthogonal polynomials (such as the Legendre polynomial), to construct the higher-order accurate solution within an element, which alleviates the above-mentioned large-stencil difficulties of the FV. Thus, an arbitrary higher-order scheme can be derived by utilizing only the von Neumann neighbourhood elements. For simplicity of the presentation, we consider one-dimensional scalar hyperbolic conservation law of the form:

$$\frac{\partial U(x,t)}{\partial t} + \frac{\partial F(x,t)}{\partial x} = 0 \tag{1}$$

where, $U(x,t)$ and $F(x,t)$ are the vectors of conservative variables and fluxes, respectively. The weak form of the DG method can be obtained multiplying Eq. (1) on the *l*-th order discontinuous basis function $w_l(x)$ and integrating over the element:

$$\begin{aligned} &\int_{x_{i-1/2}}^{x_{i+1/2}} dx w_l(x)\left[\frac{\partial U(x,t)}{\partial t} + \frac{\partial F(x,t)}{\partial x}\right] = \\ &\int_{x_{i-1/2}}^{x_{i+1/2}} dx w_l(x)\frac{\partial U(x,t)}{\partial t} - \int_{x_{i-1/2}}^{x_{i+1/2}} dx F(x,t)\frac{\partial w_l(x)}{\partial x} \\ &+ w_l(x)\hat{F}(x,t)|_{x_{i+1/2}} - w_l(x)\hat{F}(x,t)|_{x_{i-1/2}} \end{aligned} \tag{2}$$

where $\hat{F}$ is the numerical flux. The hierarchical (orthogonal) basis functions are commonly used in order to produce the diagonal mass matrix. For example, if the (scaled) Legendre polynomials $P_l(x)$ are chosen, then Eq. (2) becomes:

$$\begin{aligned} &\frac{dU_l(t)}{dt} - \frac{2l+1}{\Delta x}\Big[\int_{x_{i-1/2}}^{x_{i+1/2}} dx F(x,t)\frac{dP_l(x)}{dx} \\ &+ P_l(x)\hat{F}(x,t)|_{x_{i+1/2}} - P_l(x)\hat{F}(x,t)|_{x_{i-1/2}}\Big] = 0 \end{aligned} \tag{3}$$

Eq. (3) is integrated over the time interval [t_n, t_{n+1}] to yield discretized nonlinear residual functions:

$$\begin{aligned} &Res(U^{n+1}) = U_l^{n+1} - U_l^n + \\ &\frac{(2l+1)\gamma\Delta t}{\Delta x}\left[\int_{x_{i-1/2}}^{x_{i+1/2}} dx F(x,t)\frac{dP_l(x)}{dx} + \right. \\ &\left. + P_l(x)\hat{F}(x,t)|_{x_{i+1/2}} - P_l(x)\hat{F}(x,t)|_{x_{i-1/2}}\right] \end{aligned} \tag{4}$$

where $\gamma = 1$ and $\frac{1}{2}$ for backward Euler and Crank-Nicholson schemes, correspondingly*.

The Newton-Krylov (NK) method is a synergetic combination of the Newton method and Krylov subspace iteration methods. At each step of the Newton iteration, we must solve the linear system of equations of the form:

$$\mathbb{J}^k \delta U^k = -Res(U^k) \tag{5}$$

where $\mathbb{J}^k$ is the Jacobian matrix of the k^{th} Newton step. The linear system (5) is solved using a Krylov method (commonly, GMRES), and the solution is updated as

$$U^{k+1} = U^k + \delta U^k \tag{6}$$

The JFNK takes advantage of the fact that Krylov methods involve only simple matrix-vector product operations and do not require explicit form of the Jacobian matrix. The matrix-vector product $\mathbb{J}v$ can then be approximated by the finite difference version of the directional (Gâteaux) derivative as (Brown and Saad, 1990):

$$\mathbb{J}v \approx \frac{Res(U + \epsilon v) - Res(U)}{\epsilon} \tag{7}$$

where ϵ is a small perturbation parameter. Thus, for solving the discrete system Eq.(5), we need only nonlinear residual function Eq.(4) evaluations.

3. Physics-based preconditioning

The key to success of the JFNK is an efficient preconditioning of the GMRES. The right-preconditioned system can be expressed as

$$\mathbb{J}^k \mathbb{M}^{-1} (\mathbb{M} \delta U^k) = -Res(U^k) \tag{8}$$

where $\mathbb{M}$ is the preconditioning matrix or algorithm. The matrix-vector product of the above system can be approximated by

$$\mathbb{J}\mathbb{M}^{-1} v \approx \frac{Res(U + \epsilon \mathbb{M}^{-1} v) - Res(U)}{\epsilon} \tag{9}$$

*For details of implicit Runge-Kutta residual evaluations see (Nourgaliev et al., 2008).

Physics-based preconditioning (PBP) techniques are widely used for solving non-linear systems (Knoll et al., 2005), (Mousseau et al., 2004), (Reisner et al., 2005). The preconditioning step can be viewed as the equivalent procedure to approximating the new time step solution by a simpler (and less expensive) method. Here, a classical operator-splitting or semi-implicit discretization will be utilized as the PBP for the JFNK. An effective selection of the PBP can substantially reduce the number of Krylov vectors, which consequently reduces both the memory requirement and computational effort.

3.1. Operator-split physics-based preconditioner

The conservative form of the Navier-Stokes equations is:

$$\begin{aligned} &\frac{\partial \rho}{\partial t} + \frac{\partial \rho u}{\partial x} = 0 \\ &\frac{\partial \rho u}{\partial t} + \frac{\partial \left(\rho u^2 + p\right)}{\partial x} - \frac{\partial}{\partial x}\left(\mu \frac{\partial u}{\partial x}\right) = 0 \\ &\frac{\partial E}{\partial t} + \frac{\partial u(E+p)}{\partial x} - \frac{\partial}{\partial x}\left(u\mu \frac{\partial u}{\partial x}\right) - \frac{\partial}{\partial x}\left(\beta \frac{\partial i}{\partial x}\right) \end{aligned} \tag{10}$$

where ρ, u, E, p, i, μ and $\beta = \frac{\kappa}{C_v}$ are density, velocity, total energy, pressure, internal energy, viscosity, and the ratio of conductivity κ to specific heat C_v, respectively. In practical applications we are interested in following material velocity time scales accurately, but we would like to step over other (faster) time scales due to stiff pressure waves, viscous dissipation and heat conduction. Therefore, at the preconditioning step, we would like to solve Eq.(10) in an approximate form. Traditional semi-implicit methods (Harlow and Amsden, 1971) or operator-split (OS) segregated solution algorithms can be used for this purpose. We would like to perform the preconditioning step in the primitive variables (pressure, velocity, internal energy), where the separation of physical phenomena is more transparent.

It is important to maintain some consistency in discretization between the original and the preconditioning system. In this regard we introduce the following similarity transformation, converting the original conservative formulation to the primitive variable form.

$$\mathbb{A}^{-1} \mathbb{J}^k \mathbb{A} \delta V^k = -\mathbb{A}^{-1} \mathrm{Res}(U^k) \tag{11}$$

$$\tilde{\mathbb{J}}\delta V^k = -\mathrm{Res}(V^k) \tag{12}$$

where δV represents the vector of primitive variables, $\tilde{\mathbb{J}}$ is the Jacobian matrix in the primitive variables and $\mathbb{A}$ and $\mathbb{A}^{-1}$ are the transformation matrices of the form:

$$\mathbb{A} = \begin{pmatrix} \frac{\partial \rho}{\partial p} & \frac{\partial \rho}{\partial u} & \frac{\partial \rho}{\partial i} \\ \frac{\partial u}{\partial p} & \frac{\partial m}{\partial u} & \frac{\partial m}{\partial i} \\ \frac{\partial E}{\partial p} & \frac{\partial E}{\partial u} & \frac{\partial E}{\partial i} \end{pmatrix} \tag{13}$$

$$\mathbb{A}^{-1} = \begin{pmatrix} \frac{\partial p}{\partial \rho} & \frac{\partial p}{\partial m} & \frac{\partial p}{\partial E} \\ \frac{\partial u}{\partial \rho} & \frac{\partial u}{\partial m} & \frac{\partial u}{\partial E} \\ \frac{\partial i}{\partial \rho} & \frac{\partial i}{\partial m} & \frac{\partial i}{\partial E} \end{pmatrix} \tag{14}$$

The linear system Eq. (12) can be expressed in the following block-matrix form:

$$\begin{pmatrix} \mathbb{J}_{pp} & \mathbb{J}_{pu} & \mathbb{J}_{pi} \\ \mathbb{J}_{up} & \mathbb{J}_{uu} & \mathbb{J}_{ui} \\ \mathbb{J}_{ip} & \mathbb{J}_{iu} & \mathbb{J}_{ii} \end{pmatrix} \begin{pmatrix} \delta p \\ \delta u \\ \delta i \end{pmatrix} = \begin{pmatrix} Res_p \\ Res_u \\ Res_i \end{pmatrix} \tag{15}$$

In the low-Mach number limit ($u \ll c$), we can linearize the material velocity (u) at the previous Newton step and Eq. (15) can be simplified to:

$$\begin{pmatrix} \mathbb{J}_{pp} & \mathbb{J}_{pu} & \mathbb{J}_{pi} \\ \mathbb{J}_{up} & \mathbb{J}_{uu} & \mathbb{J}_{ui} \\ 0 & 0 & \mathbb{J}_{ii} \end{pmatrix} \begin{pmatrix} \delta p \\ \delta u \\ \delta i \end{pmatrix} = \begin{pmatrix} Res_p \\ Res_u \\ Res_i \end{pmatrix} \tag{16}$$

Now, Eq. (16) can be solved in three steps:

$$\begin{aligned} &1)\ \ \delta i = \mathbb{J}_{ii}^{-1} Res_i \\ &2)\ \ \left(\mathbb{J}_{pp} - \mathbb{J}_{pu}\mathbb{J}_{uu}^{-1}\mathbb{J}_{up}\right)\delta p = \begin{pmatrix} Res_p - \mathbb{J}_{pi}\delta i \\ +\mathbb{J}_{pu}\mathbb{J}_{uu}^{-1}\mathbb{J}_{ui}\delta i \\ -\mathbb{J}_{pu}\mathbb{J}_{uu}^{-1} Res_u \end{pmatrix} \\ &3)\ \ \delta u = \mathbb{J}_{uu}\left(Res_u - \mathbb{J}_{up}\delta p - \mathbb{J}_{ui}\delta i\right) \end{aligned} \tag{17}$$

The Schur complement matrix that appears in the Step 2) can be approximated by $\left(\mathbb{J}_{pp} - \mathbb{J}_{pu}\tilde{\mathbb{J}}_{uu}^{-1}\mathbb{J}_{up}\right)$, where $\tilde{\mathbb{J}}_{uu}$ is the diagonal-reduced-form of $\mathbb{J}_{uu}$.

4. Numerical results

In this section, we utilize our JFNK-DG framework to solve one- and two-dimensional conservative form of Navier-Stokes equations. In the first example, we demonstrate the high-order convergence rate of the JFNK-DG using the method of manufactured solutions (Knupp et al., 2003). The following solution is manufactured:

$$\begin{aligned} \rho(x,t) &= \rho_{\min} + (\rho_{\max} - \rho_{\min})\,\mathrm{sech}\left(\frac{x - U_{int}t}{\delta}\right) \\ P(x,t) &= P_{\min} \\ &\quad + \frac{\Delta P_0}{2}\left(1 + \tanh\left(\frac{x - U_{int}t}{\delta}\right)\right) \\ &\quad + \frac{\Delta P_1}{2}\left(1 + \tanh\left(\frac{x - C_1 t}{\delta_1}\right)\right) \\ u(x,t) &= U_0 + (U_{int} - U_0)\left(1 + \tanh\left(\frac{x - U_{int}t}{\delta}\right)\right) \end{aligned} \tag{18}$$

Fig. 1a shows the results of the convergence tests using the 1st (DG_0) to 4th (DG_3) order DGs. Consistency of the computed and theoretical convergence rates is evident for all cases. Note, that in the abscissa of the Fig. 1a, we show the total number of degrees of freedom (DOFs). It clearly shows that the higher-order methods can obtain a much more accurate result with fewer DOFs. Fig. 1b shows the convergence of the fully implicit time discretizations, which also demonstrates the consistent convergence rate.

In order to visualize the effectiveness of the developed PBP, the eigenvalues of the Jacobian matrix $\mathbb{J}$ and of the preconditioned matrix $\mathbb{J}\mathbb{M}^{-1}$ are computed. Fig.2 shows the eigenvalue distributions of the original system, the block-Jacobi, and the operator-split preconditioners. Because the Jacobian is non-symmetric, the eigenvalues are, in general, complex. A condition number of a problem is related to the spread of the eigenvalue distribution. A well-conditioned system should have eigenvalues clustered around 1. From Fig. 2 it can be seen that the minimum eigenvalue of the original system moves away from 1 as the Mach number becomes smaller. The block-diagonal (BD) preconditioned system* has more clustered eigenvalue pattern; however as the Mach number approaches zero, the

*For details of the block diagonal preconditioner see (Nourgaliev et al., 2008)

minimum eigenvalue moves away from 1. On the other hand, the operator-split preconditioner tends to collapse all eigenvalues onto the real-axis, and the distributions are almost independent of the Mach number, which implies effectiveness of the preconditioning even at the very low Mach number limit.

Fig. 3 depicts the number of GMRES iterations vs. the Mach number and Reynolds number. As we expected, the unpreconditioned and the block diagonal preconditioned GMRES have strong dependence on the Mach number and viscosity. However the number of iterations with the OS preconditioner is almost independent of both of these parameters, and able to reduce the number of iterations by more than factor of ten.

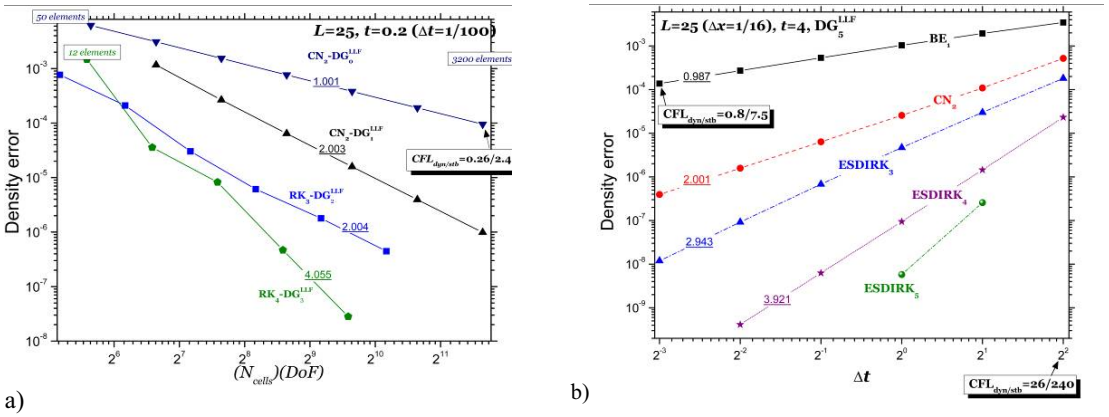

Fig. 1 Convergence test of a) Discontinuous Galerkin spatial discretization, b) high-order implicit time discretization using the method of the manufactured solutions.

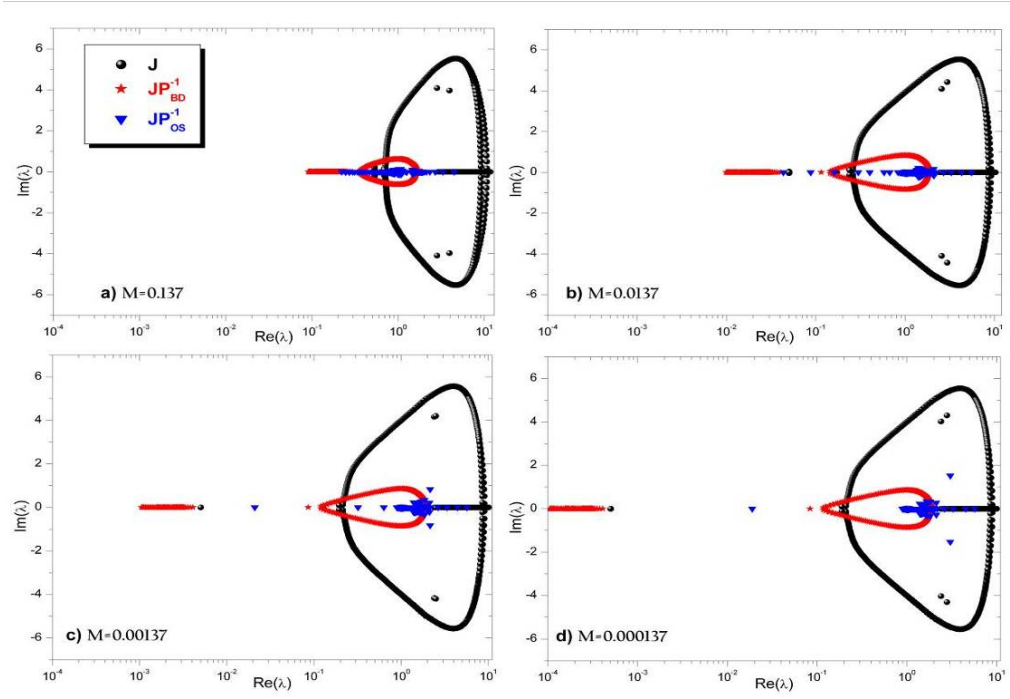

Fig. 2 Eigenvalue distributions of the original and the preconditioned system

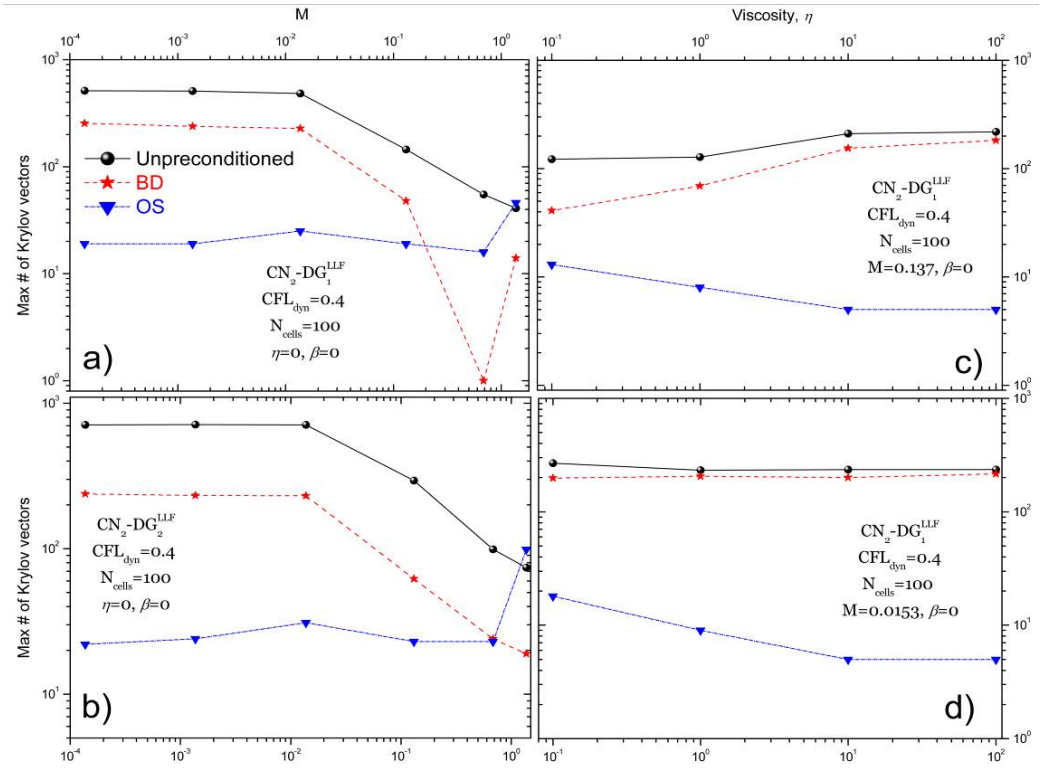

Fig. 3 The number of Krylov iterations vs. Mach number and viscosity effects

As a second example, we solved the two-dimensional "Travelling wave" problem. The velocity and pressure profiles are given by

$$u(x,y,t) = 1 + 2\cos[2\pi(x-t)]\sin[2\pi(y-t)]$$
$$v(x,y,t) = 1 - 2\sin[2\pi(x-t)]\cos[2\pi(y-t)] \quad (19)$$
$$P(x,y,t) = P_0 - \cos[4\pi(x-t)] - \cos[4\pi(y-t)]$$

P_0 and the constant initial density are set to 70.25 and 0.1, respectively; corresponding to the Mach number of 0.1. Fig, 4a shows the convergence rate for total energy using the linear and quadratic DG. The consistent convergence rates are observed for both cases. Fig. 4b shows a sample of the velocity and vorticity fields for time 0.2.

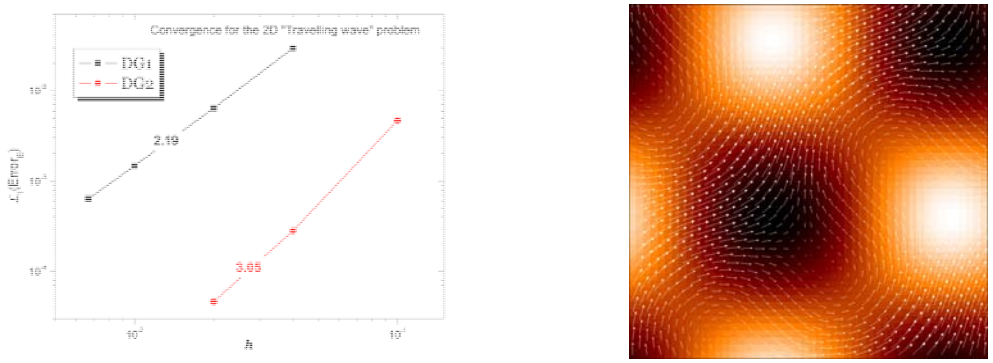

a) b)

Fig. 4 "Travelling wave" problem: (a) convergence plot for DG_1 and DG_2; b) vorticity and velocity fields at t = 0.2.

The last example is the two-dimensional thermally-driven square cavity problem (de Vahl Davis, 1983; de Vahl Davis and Jones, 1983). The problem consists of the unit square cavity with insulated horizontal walls and heated vertical walls. The flow in this problem is driven by the buoyancy forces created by the temperature difference in the wall. The steady state flow field and temperature distributions are depicted in Fig. 5a. Prandtl and Rayleigh numbers of the problem are set to 0.71 and 10^4, respectively. Temperature difference is 12K between hot and cold walls, and the maximum Mach number of the problem is found out to be $\sim 2 \cdot 10^{-4}$. We have used the rDG_0 method (Nourgaliev et al., 2008) for the spatial discretization, and Backward Euler for the temporal integration. The local Nusselt number distribution along the vertical wall is shown in Fig. 5b. Both the maximum and minimum Nusselt numbers along the vertical walls match within 0.2% of the benchmark solution given in (de Vahl Davis, 1983). This problem reaches the steady state in ~30 seconds. Table 1 compares the performance of the OS-PBP with different mesh sizes. Comparison was made around time t ~15 seconds. The number of the Krylov iterations per Newton steps slightly increases as the mesh size decreases. This is due to increase in the time step sizes.

Next, in order to perform a fair estimate of the method's performance, we consider a transient problem, by setting time-dependent temperature boundary conditions at the hot wall. Dynamics of the transient problem are shown in Fig. 6. Table 2 lists the number of iterations used to solve this transient problem under fixed CFL numbers. From this table, the effectiveness of the developed preconditioner is apparent. It is also seen to be independent of the mesh size and only weakly dependent on the CFL numbers.

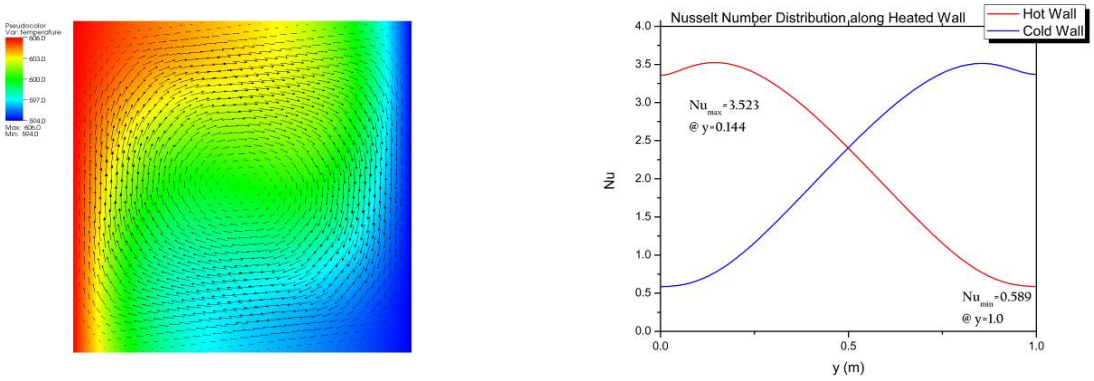

a) b)

Fig. 5 Temperature and Nusselt number distribution of the thermally driven cavity flow problem.

Table 1
Efficiency of the operator-split preconditioner in pseudo-transient problem. Simulation was carried out to physical time of 30 seconds. Time steps were adaptively changed using the time step control method introduced in (Knoll et al., 1996). The final flow field and temperature distribution are depicted in Fig. 5a.

Grid Size	Total # of time steps	Max time step size	Average #Krylov/Newton	Average #Newton/time step
64x64	2515	0.05 ($CFL_{acoustic}$≈1000)	10 ($\Delta t \approx 0.01$)	3
128x128	1060	0.05 ($CFL_{acoustic}$≈2000)	14 ($\Delta t \approx 0.025$)	4
256x256	618	0.05 ($CFL_{acoustic}$≈4000)	30 ($\Delta t \approx 0.05$)	5

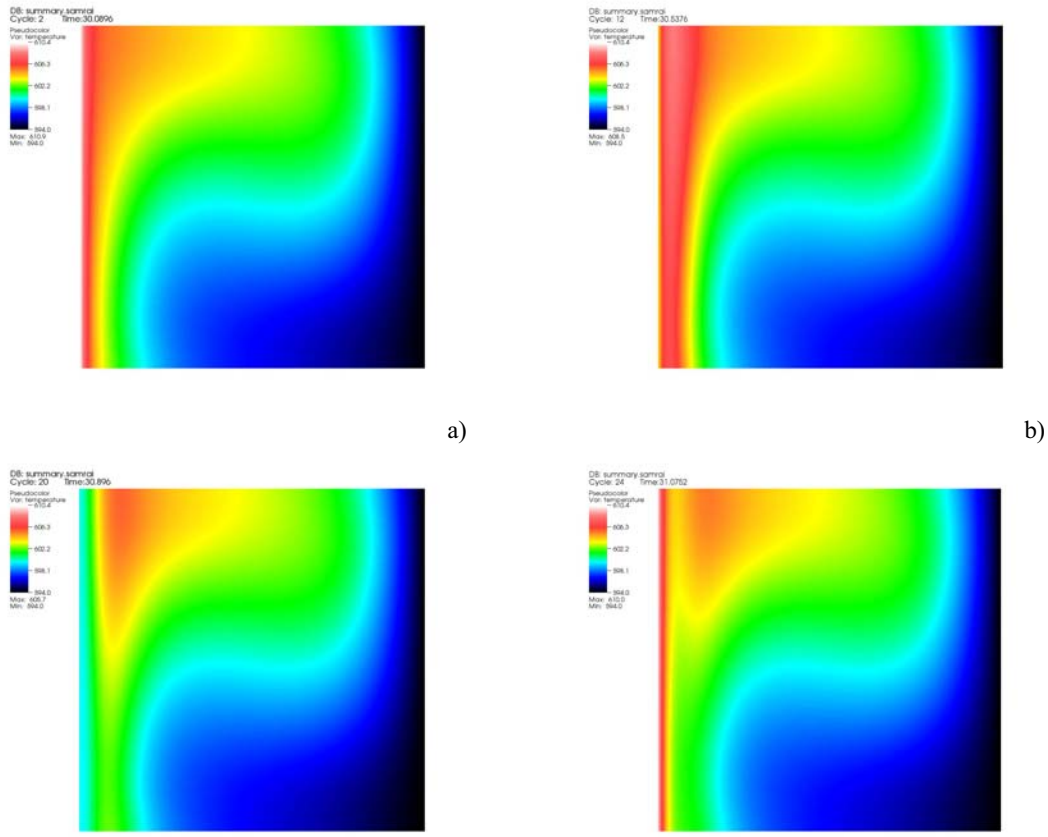

a) b)

c) d)

Fig. 6 Temperature distributions of the thermally driven cavity flow transient problem; time t = a) 0.08596, b) 0.5376, c) 0.8960, and d) 1.0752 seconds

Table 2
Efficiency of the operator split preconditioner in transient problem. Dynamics of the transient problem are depicted in Fig. 6.

Grid Size	$CFL_{acoustic} \approx 250$		$CFL_{acoustic} \approx 1000$		$CFL_{acoustic} \approx 4000$	
	#Krylov/ Newton	#Newton/ Time step	#Krylov/ Newton	#Newton/ Time step	#Krylov/ Newton	#Newton/ Time step
64x64	12.0	4.0	22.0	6.0	38.4	7.7
128x128	10.5	4.2	20.0	5.5	36.8	7.2
256x256	9.3	4.1	17.3	5.5	32.7	6.7

5. Summary

In this work, we have developed a fully implicit higher-order discontinuous Galerkin method (JFNK-DG), demonstrating its high-order grid convergence and the efficiency of the physics-based preconditioning. The numerical results show that the convergence rates are consistent with the theory, and that the effective clustering of the eigenvalues due to the physics-based preconditionings (Operator-Split and Block-Diagonal) produces a significant acceleration of the GMRES convergence. Moreover, the eigenvalue pattern of the OS preconditioner is almost independent of the Mach number, and the number of GMRES iterations are shown to be constant over a wide range of the Mach numbers and viscosities, under fixed CFL conditions.

6. Acknowledgement

Prepared for the U.S. Department of Energy Office of Nuclear Energy Under DOE Idaho Operations Office Contract DE-AC07-05ID14517 (INL/CON-08-14243)

References

Brown, P. N., and Saad, Y., 1990, Hybrid Krylov methods for nonlinear systems of equations: SIAM Journal of Science and Statistical Computing, v. 11, p. 450-480.

Cockburn, B., Hou, S., and Shu, C. W., 1990, TVB Runge-Kutta local projection discontinuous Galerkin finite element method for conservation laws IV: The multidimensional case: Mathematics of Computation, v. 54, p. 545-581.

Darbandi, M., and Hosseinizadeh, S. F., 2007, Numerical study of natural convection in vertical enclosures using a novel non-Boussinesq algorithm: Numerical heat Transfer Part A: Applications, v. 52, p. 849-873.

de Vahl Davis, G., 1983, Natural Convection of Air in a Square Cavity: A Benchmark Numerical Solution: International Journal for Numerical Methods in Fluids, v. 3, p. 249-264.

de Vahl Davis, G., and Jones, I. P., 1983, Natural Convection in a Square Cavity: A Comparison Exercise: International Journal for Numerical Methods in Fluids, v. 3, p. 227-248.

Harlow, F. H., and Amsden, A. A., 1971, A Numerical Fluid Dynamics Calculation Method for All Flow Speeds: Journal of Computational Phys, v. 8, p. 197-213.

Knoll, D. A., and Keyes, D., 2004, Jacobian-free Newton-Krylov Methods: A Survey of Approaches and Applications: Journal of Computational Physics, v. 193, p. 357-397.

Knoll, D. A., McHugh, P. R., and Keyes, D. E., 1996, Newton-Krylov Methods for Low-Mach-Number Compressible Combussion: AIAA Journal, v. 34, p. 961.

Knoll, D. A., Mousseau, V. A., Chacon, L., and Reisner, J. M., 2005, Jacobian-Free Newton-Krylov Methods for the Accurate Time Integration of Stiff Wave Systems: Journal of Scientific Computing, v. 25, p. 213-230.

Knupp, P. M., Salari, K., and Krantz, S. G., 2003, Verification of Computer Codes in Computational Science and Engineering,, CRC Press.

Mousseau, V. A., Knoll, D. A., and Rider, W. J., 2004, New Physics-based preconditioning of Implicit Methods for Nonequilibrium Radiation Diffusion: Journal of Computational Phys, v. 190, p. 104-132.

Nourgaliev, R. R., Theofanous, T. G., Park, H., Mousseau, V., and Knoll, D., 2008, Direct Numerical Simulation of Interfacial Flows: Implicit Sharp-Interface Method (I-SIM). 46th AIAA Aerospace Sciences Meeting and Exhibit, Reno, NV.

Pope, M. A., and Mousseau, V. A., 2007, Accuracy and Efficiency of a Coupled Neutronics and Thermal Hydraulics Model: The 12th international Topical Meeting on Nuclear Reactor Thermal Hydraulics.

Reisner, M., Mousseau, V. A., Wyszogrodzki, A. A., and Knoll, D. A., 2005, A Fully Implicit Hurricane Model with Physics-based Preconditioning: Monthly Weather Review, v. 133, p. 1003-1022.